Proceedings World Geothermal Congress 2015
Melbourne, Australia, 19-25 April 2015

New Approaches of Coupled Simulation of Deep Geothermal Systems

Guido Blöcher[1], Mauro Cacace[1], LiWah Wong[1], Oliver Kastner[1], Günter Zimmermann[1], Ernst Huenges[1], Norihiro Watanabe[2] and Olaf Kolditz[2]

[1]Helmholtz-Zentrum Potsdam - Deutsches GeoForschungsZentrum GFZ

[2]Helmholtz Centre for Environmental Research – UFZ

guido.bloecher@gfz-potsdam.de

Keywords: Tetrahedralization, Meshing, Faulted, Coupled Simulation, Geothermal Systems

ABSTRACT

Determining flows, heat transfer and reactive transport processes in natural faulted and fractured geological systems receives increasing attention. Efforts are not only restricted to a better geological characterization of the complex geometry of the faulted and fractured rock reservoirs but also to describe the actual geometry and to simulate the dynamics of flow and transport processes in these natural systems. In this paper, a technical description of an improved method is presented to represent non-planar structures of deviated wells (1D) and faults and fractures (2D) within a boundary conforming Delaunay unstructured mesh (3D).

The main advantage of this approach is that these dipping structures can be integrated into a 3D volume representing the hosting porous matrix. Consequently, the interaction between the discrete flow paths through and across faults and fractures and within the rock matrix can be correctly simulated. The crucial factor that makes the approach applicable to real case geological systems is that all algorithms are parallel thus computing time increase approximately linearly with data volumes.

This approach is presented in terms of a real case study of the deep geothermal reservoir of Groß Schönebeck in the North of Berlin, Germany. The model domain includes six major geological units, three major fault zones and a doublet system consisting of four induced hydraulic fractures. This domain was triangulated resulting in 6,191,564 tetrahedra and subsequently used for dynamic simulation.

1. INTRODUCTION

Many petroleum, gas, geothermal, and water supply reservoirs form in fractured and faulted rock systems (Committee on Fracture Characterization and Fluid Flow, National Research Council, 1996). The presence of discrete heterogeneities in the underground controls the flow and transport into and through the subsurface (Berkowitz, 2002). Faults and fractures can act as either preferentially hydraulic conductors or hydraulic barriers (Davatzes and Aydin, 2005).

There exist different approaches for numerical studies of flow and transport processes in fractured media neglecting the matrix contribution (Bear et al., 1993). One class of such approaches comprises discrete fracture models in which fracture characteristics (e.g. dimension, orientation, apparent aperture and density) are designed to reflect physical properties as obtained by different geophysical monitoring methodologies (Trice, 1999). Discrete network models usually assume flow to take place only within the fracture planes or through fracture-fracture interconnections (Cacas et al., 1990). Though neglecting the permeability of the porous matrix is a feasible assumption in specific groundwater studies (Deshowitz, 1985), the importance of matrix diffusion cannot be neglected in studies involving energy and solute transport (Grisak and Pickens, 1980).

For an example, reservoir management (Ahmed and Meehan, 2011) requires detailed knowledge of the reservoir behaviour and of the overall system including the geological units of interest, the major fault zones, the natural and induced fractures, and the production and injection wells. A numerical simulation of processes occurring in such systems provides useful tools for basic process understanding and for improving prediction capabilities (Kolditz et al., 2010). A real case based on a numerical application relies on a number of geophysical data which are collected in the field and organized into consistent 3D geological models of the reservoir (Caumon et al., 2009; Farmer, 2005). In order to carry out a dynamic simulation a gridding or unstructured meshing of the 3D geological model is required. Commercial software now exist which provide built-in modules to generate grids (e.g. EarthVision (Chen et al., 2013)) and unstructured meshes (Gocad (Prévost et al., 2005) and Petrel (Souche et al., 2013)) suitable for reservoir dynamic simulations.

Common to all reservoir models is to deal with geometries of different spatial scales and dimensions, e.g. 0D injection/production points, 1D wells, 2D fractures and faults, and 3D reservoir rocks. To represent these features with a tolerable amount of discrete elements a superposition of lower dimensional elements onto higher dimensional elements is required, as seen in Figure 1. This method is referred to as the common node approach (Therrien and Sudicky, 1996; de Rooij, 2008). Earlier studies relied on orthogonal grids in which discrete fractures were aligned with one dimensional faces of grid elements (Shikaze et al., 1998). More recent ones have tried to either include 2D fracture elements as additional geometric constraints to the vertical and horizontal elements of the matrix (Graf and Therrien, 2008; Normani and Sykes, 2010) or couple high resolution 2D fracture models with 3D matrix models (Blessent et al., 2009). So far, no attempt has been made to integrate the open hole section of a well into discrete unstructured meshes.

The major complication of such an approach is to maintain the internal geometric consistency between well, fault, and matrix elements. This requires each well element to be mapped onto a 1D edge and each fault element to be mapped onto a 2D face of at least a single 3D matrix element, see Figure 1. Fully respecting the input geological structure can lead to numerical meshes having

badly shaped wedges of the rock volume or non-conforming volumes in the vicinity of fault offsets. Some methodologies exist to overcome such complications though they are mainly restricted to 2D problems (Mustapha and Dimitrakopoulos, 2011; Holm et al., 2006).

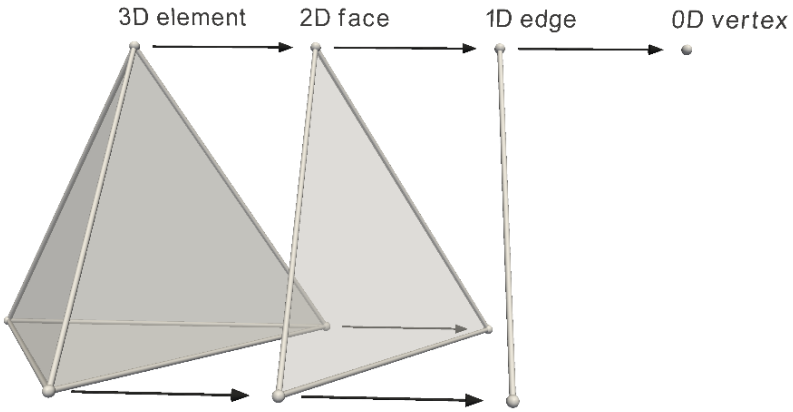

Figure 1: Schematic illustration of the common node approach: superposition of 0D (e.g. source/sink point), 1D (e.g. well path) and 2D (e.g. faults) elements onto 3D elements of the porous matrix.

In the following paragraphs, a description of an automated method to represent 1D polylines and 2D non-planar structures of generic inclines within a 3D boundary conforming Delaunay unstructured mesh is outlined. We will show how fundamental geometric concepts can be used to bridge the gap between geological and dynamic forward models of flow and to transport processes in rock domains comprising fault zones. The approach has been already successfully tested for both synthetic (Blöcher et al., 2010a; Cherubini et al., 2013) and realistic case studies (Cacace et al., 2013; Hofmann et al., 2014).

2. STRUCTURAL SETTING AND MESH GENERATION

Combining fundamental algorithms from computational geometry and Delaunay triangulations (Shewchuk, 2002), an automated approach has been developed to generate piecewise linear complexes from geological models of faulted reservoirs. A constrained Delaunay tetrahedralization (Si, 2008) is performed on the generated piecewise linear complex resulting in an unstructured tetrahedral mesh suitable for dynamic simulations.

In the improved technique, wells are discretized as 1D poly-lines and faults are discretized as 2D triangular surfaces embedded into a 3D unstructured mesh of the rock matrix. The two essential features of the novel methodology are (1) the way geological information are updated to offer fast and efficient modification of the system geometry; and (2) the imaging of discrete flow paths within the porous rock matrix.

In this study, we investigated the deep geothermal reservoir of Groß Schönebeck (north of Berlin, capital city of Germany). The reservoir is located between -4050 and -4250 m depth in the Lower Permian sedimentary rocks of the Northeast German Basin, as seen in Figure 2. It consists of 6 geological units, three internal fault zones, and four existing hydraulically induced fractures (three at the production well (Zimmermann et al., 2010) and one at the injection well (Zimmermann et al., 2009)). The fault pattern is characterized by major NW-striking faults and NNE-striking minor fault having no significant offset. The model area has an extent of 5448 m in east-west and 4809 m in north-south direction with the maximum vertical extension of 594 m (Blöcher et al., 2010b). Furthermore, the model domain is constrained by two major fault zones in SW and NE acting as no-flow barriers and two additional borders in SE and NW closing the volume domain. The fracture half-lengths vary between 60 m and 190 m and the fracture height varies between 95 m and 145 m.

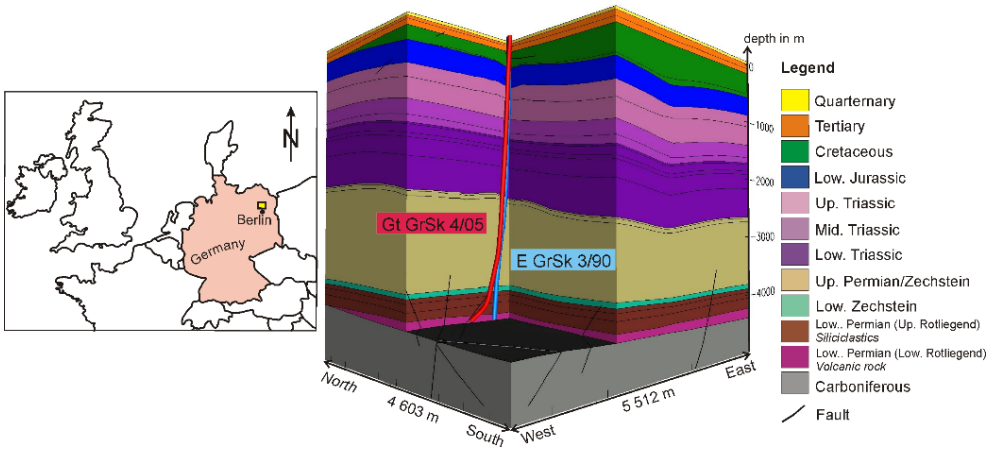

Figure 2: Location of the research drill site (left) and 3D view of the two research wells and the geological horizons (Blöcher et al., 2008, modified).

In order to represent all these features, the minimum and maximum lengths were set to 8 m and 16 m, respectively. This results in 6,191,564 tetrahedra and 1,058,866 vertices representing the six geological units. Material identifiers were set to all units, faults and fractures, and the production well (Figure 3). Marked faults and fractures are represented by 835,959 triangles which have been included in the final tetrahedral mesh. The production well is represented by 73 edges having their own material identifier. Computation of all convex hulls, triangulation of the surfaces, and all intersection poly-lines takes 22,202 seconds (approximately 6.2 hours). The subsequent performed constrained Delaunay triangulation and constrained Delaunay tetrahedralization takes additionally 1,072 seconds.

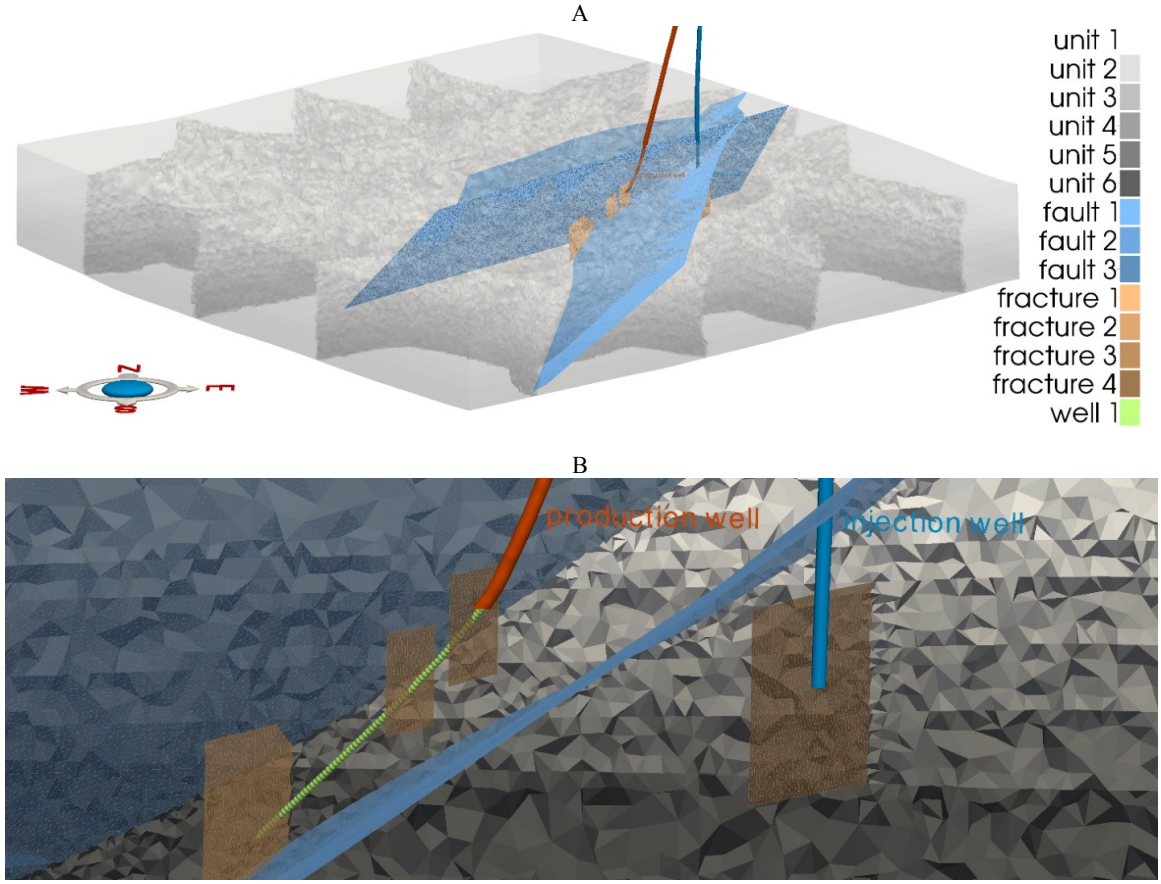

Figure 3: Case study of the deep geothermal reservoir of Groß Schönebeck northern Germany (Blöcher et al., 2010b). This domain was triangulated resulting in 6,191,564 tetrahedra representing the units, 835,959 faces representing the faults and fractures and 73 edges representing the well (Figure 3B). A multiparallel simulation was conducted over 24 cores indicated by the subdomains (Figure 3A).

3. SIMULATION

Numerical simulations were conducted using OpenGeoSys (OGS) which is a scientific open-source initiative for numerical simulation of thermo-hydro-mechanical/chemical processes in porous media (www.opengeosys.org; Watanabe et al., 2012; Kolditz et al., 2012). OGS is primarily based on the finite element method and offers a hybrid approach combining discrete fracture and continua models for simulating flow and transport processes in fractured rocks.

To simulate the lifecycle performance during 100 years of production and injection, a steady state simulation and a subsequent transient one were performed. With the steady state simulation the in situ pressure, temperature, and velocity field was calculated without any withdraw from the reservoir. Based on the resulting pressure and temperature field, a transient simulation of 100 years having a production and injection rate of 18 m³/h was performed.

For in situ pressure and temperature field a hydrostatic boundary condition on each of the 4 vertical borders was applied. To calculate the pressure at certain depth, a density of 1148 kg/m³ was assumed. Furthermore, a temperature gradient of 28 °C/km was applied on the top surface. In order to simulate the terrestrial heat flux from the bottom, we set a value of 72 mW/m² at the bottom surface. The same gradients as applied for the pressure and temperature boundary conditions were used to set the initial conditions for the total domain.

To obtain the impact of varying fluid density ρ [kg/m³] and viscosity μ [Pa*s], fluid density is related to temperature T [°C], pressure p [Pa], salinity concentration C [kg/m³], and reference density ρ_0 [kg/m³]:

$$\rho = \rho_0 \left(1 - \beta(T - T_0) + \gamma(p - p_0) + \frac{\alpha}{C_s - C_0}(C - C_0) \right)$$

with thermal expansion coefficient β [°C^{-1}], compressibility γ [Pa^{-1}], and density ratio α [-], all related to temperature, pressure, and concentration (Magri et al., 2005). C_0 and C_s denote the reference concentration and the maximum concentration, respectively. The dynamic viscosity of the fluid is regarded as a function of salinity concentration and temperature T (Diersch, 2002), expressed with the mass fraction ω [-] and relative temperature coefficient ς [-]:

$$\frac{\mu_0}{\mu} = \frac{1 + 0.7063\varsigma - 0.04832\varsigma^3}{1 + 1.85\omega - 4.1\omega^2 + 44.5\omega^3};\ \omega = \frac{C}{\rho};\ \varsigma = \frac{T - 150}{100}$$

The porous media properties were used in accordance with Blöcher et al. (2010a). There, the permeability varied between 4.9346x10^{-17} m² and 1.28 x10^{-15} for the least and most conductive horizons, respectively. For the reservoir section a porosity of 0.15 was assumed which decreases to less than 0.001 for the conglomerates and volcanic rocks at the bottom of the model domain. The dimensions and hydraulic properties of the induced fractures under in situ conditions were estimated from field tests. An average aperture of 2.28 x10^{-4} m and a permeability of 2.33 x10^{-9} m² were used for all of them.

For the implemented three fault zones a sensitivity analysis was performed changing the fault zone thickness and the permeability by six orders of magnitude. This sensitivity analysis is not part of the current paper and the results corresponding to one virtual scenario (thickness of 1 m and a permeability of 1 x10^{-9} m²) are presented.

For the transient simulation, the results of the steady state simulation regarding the pressure and temperature fields were used as the initial conditions. In addition, an injection rate of 18 m³/h was applied at the center of the hydraulic induced fracture at the injection well. The production rate of 18 m³/h was applied at the top of the well section of the production site. Due to the common node approach the inflow quantities of the three hydraulic induced fractures can be calculated. To do so, six observation points were set on the well path. For each hydraulic induced fracture we measured the flow velocity shortly before and after its intersection with the well path. Knowing the cross sectional area of the well, we calculated the inflow fraction of the individual hydraulically induced fracture. For calculating the dynamic density and viscosity values (Figure 4), the same equations of state were used as for the steady state simulation. Furthermore, all properties regarding the geological units, hydraulic induced fractures, and fault zones were not altered. In order to simulate the life cycle performance of these geothermal doublet systems, a minimum simulation time of 30 years was required which we extended to 100 years to see the thermal break through time.

A

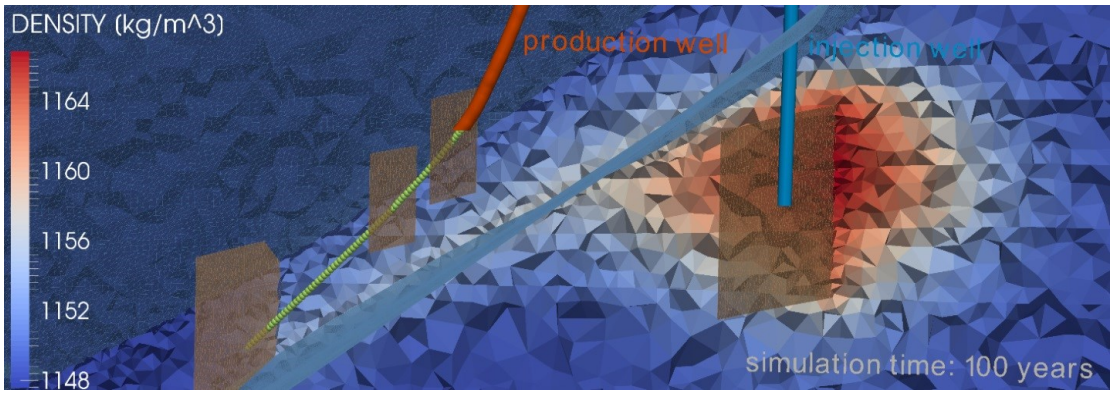

B

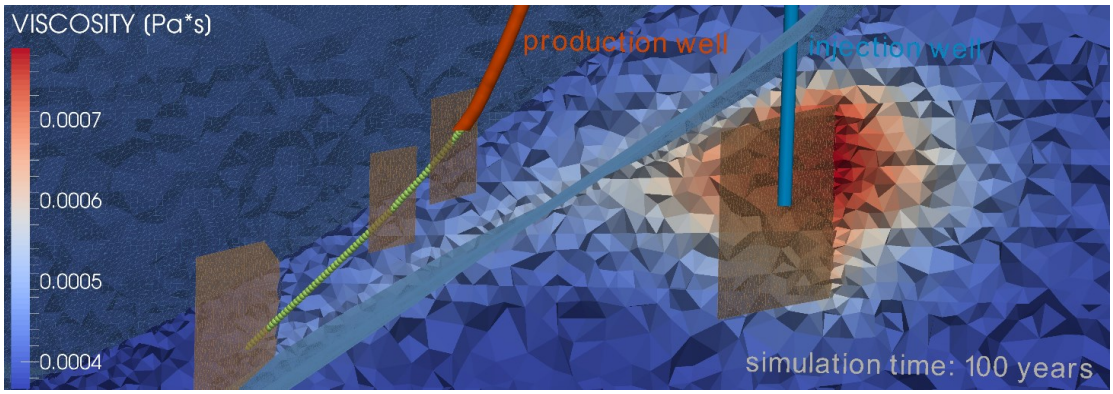

Figure 4: Calculated dynamic density (A) and viscosity (B) of the fluid depending on temperature, pressure and Total Dissolved Solids (TDS).

4. RESULTS

We calculated the fractional influx of the three hydraulic induced fracture at the production well with corresponding velocity magnitudes and the productivity index (PI [m³/h/MPa]) and injectivity index (II [m³/h/MPa]) of the production and injection well,

respectively. The productivity index can be calculated by the maximum drawdown generated Δp [MPa] by a constant flow rate $\dot{V}$ [m³/h]:

$$PI = \frac{\dot{V}}{\Delta p}$$

The injectivity index can be calculated similar taking into account a constant flow rate and the maximum buildup. At the production well the drawdown becomes quasi steady state after 2 days simulation time. It has a value of 0.8 MPa, which increases to 0.87 MPa after 100 years simulation time (Figure 5A). This drawdown correlates to a PI of 20.7 m³/h/MPa. This PI is 10 times higher than the PI measured in the field and is due to the influence of a high conductive fault zone which is connected via the induced fractures to the production well. The injection well is not connected to the high conductive fault zone. Therefore, the pressure is increasing by 7.2 MPa after 100 years. Since the viscosity increases due to injection, no quasi steady state could be observed. The corresponding II is 2.5 m³/h/MPa. This value is in the range of the measured quantities.

A

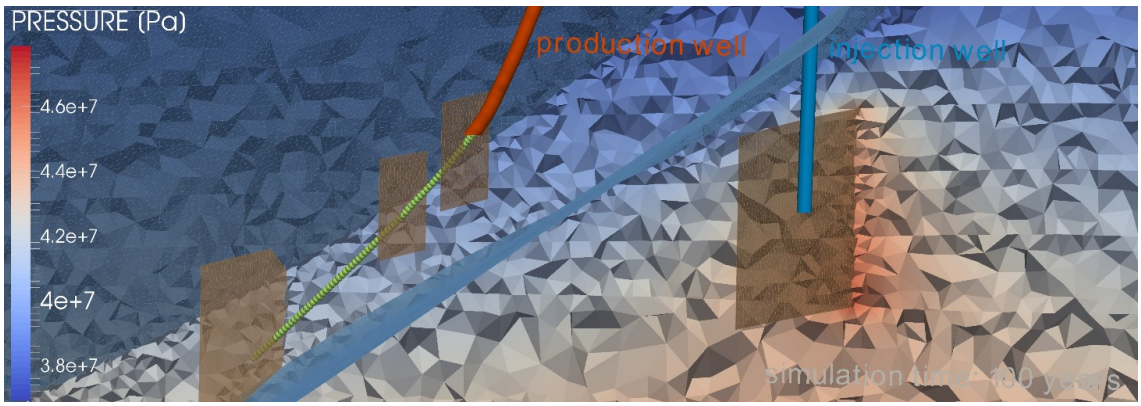

B

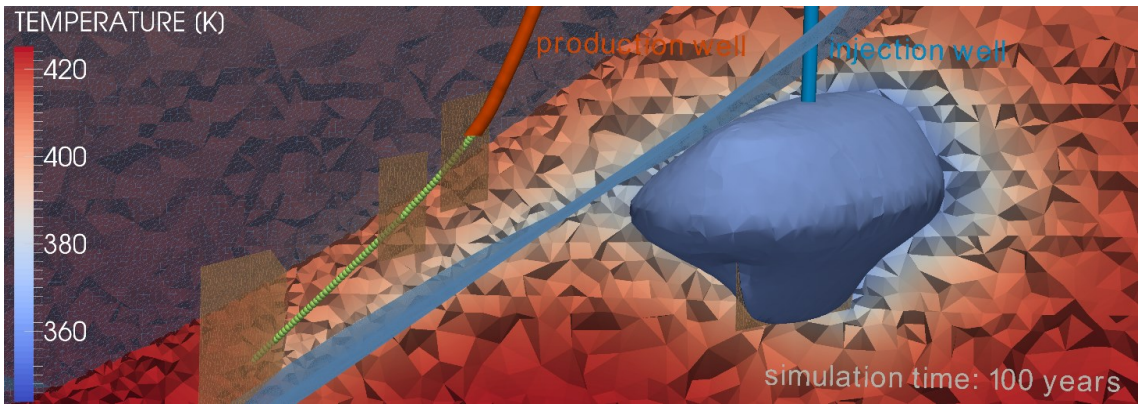

C

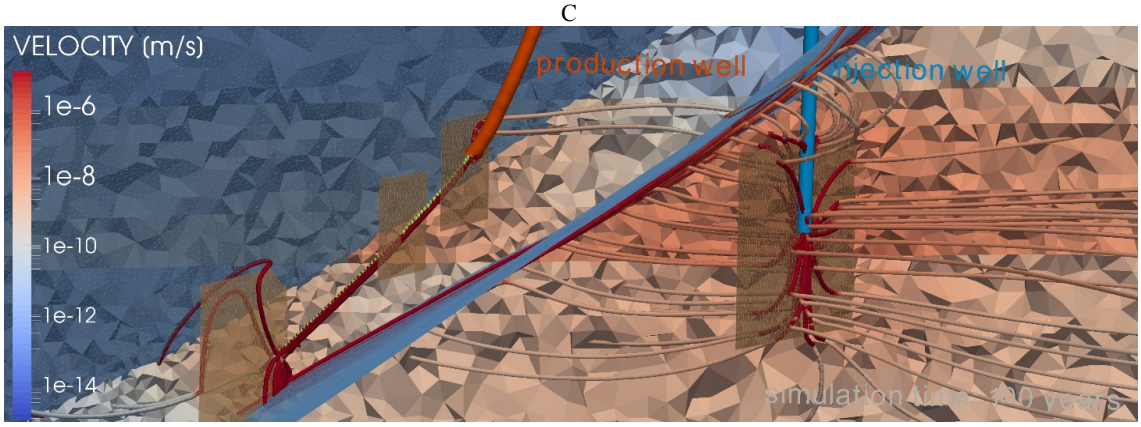

Figure 5: Simulation results showing (A) pressure distribution, (B) temperature distribution and (C) velocity field at the final simulation state at 100 years.

To calculate the influx fraction of the three hydraulic induced fractures, we measured the velocity inside the well before and after its intersection with the hydraulic induced fracture (Figure 5C). Based on the cross-sectional area the volume flux could be

calculated. Assuming a constant volume flux of 18 m³/h at the top of the well, the following quantities could be derived: 44.4% influx from the fracture in the volcanic rocks (bottom); 15.3% influx from the first gel/proppant fracture (middle) and 13.8% influx from the second gel/proppant fracture (top). The remaining 26.5% are produced from the open hole section which is situated in between the hydraulic induced fractures. These values do not correspond with the measured quantities. The measured quantities are as follows: 25% influx from the fracture in the volcanic rocks (bottom); 65% influx from the first gel/proppant fracture (middle) and 10% influx from the second gel/proppant fracture (top). Therefore, the calculated influxes are due to the assumption of a high conductive fault zone which is connected to the fracture in the volcanic rocks.

Due to the relatively low production and injection rate, no significant thermal break through could be observed. Although the highest velocities can be observed along the hydraulic induced fractures, the fault zones, and inside the well, the injected water is heated up along its way from the injection to the production point (Figure 5B). Therefore, the production temperature starts decreasing after 30 years and reaches its minimum at the end of the simulation. The maximum measured temperature drawdown is about 4°C.

5. CONCLUSION

The current study describes the generation of tetrahedral meshes suitable for finite element simulation taking structural geological data as the input structure. One case study of high complexity has been presented which has been further used for dynamic simulations as the published in separate publications (Cacace and Blöcher, 2012; Cacace et al., 2013; Hofmann et al., 2014). This case study includes wells, fractures, fault zones, and geological units. Based on these geometries a mesh with more than 6,000,000 elements has been generated. Based on this mesh, a hydraulic-thermal coupled simulation was performed subsequently. We showed that the common node approach is suitable to represent the complete structure and the relevant processes occurring in a geothermal doublet system.

REFERENCES

Ahmed, T. & Meehan, N.: (Eds.) Advanced Reservoir Management and Engineering, *Gulf Professional Publishing*, (2011), 712

Bear, J., Tsang, C.-F. & Marsily, G. D.: (Eds.) Flow and Contaminant Transport in Fractured Rock, *Academic Press*, (1993).

Berkowitz, B.: Characterizing flow and transport in fractured geological media: A review, *Advances in Water Resources*, **25**, (2002), 861 - 884.

Blessent, D., Therrien, R. & MacQuarrie, K.: Coupling geological and numerical models to simulate groundwater flow and contaminant transport in fractured media, *Computers & Geosciences*, **35**, (2009), 1897 - 1906.

Blöcher, M. G., Cacace, M., Lewerenz, B. & Zimmermann, G.: Three dimensional modelling of fractured and faulted reservoirs: Framework and implementation, *Chemie der Erde - Geochemistry*, **70**, Supplement 3, (2010a), 145 - 153.

Blöcher, M. G., Reinicke, A., Moeck, I., Milsch, H. & Zimmermann, G.: Concept of a Hydro-Mechanical-Thermal Simulation of a Fractured Reservoir. *42nd US Rock Mechanics Symposium and 2nd U.S.-Canada Rock Mechanics Symposium*, San Francisco, June 29-July 2, (2008), 1-8.

Blöcher, M. G., Zimmermann, G., Moeck, I., Brandt, W., Hassanzadegan, A. & Magri, F.: 3D numerical modeling of hydrothermal processes during the lifetime of a deep geothermal reservoir, *Geofluids*, **10**, (2010b), 406-421.

Cacace, M., Blöcher, G.: Modelling of 3D fractured geological systems - technique and applications, *34th International Geological Congress (IGC)*, Australia, (2012).

Cacace, M., Blöcher, G., Watanabe, N., Moeck, I., Börsing, N., Scheck-Wenderoth, M., Kolditz, O. & Huenges, E.: Modelling of fractured carbonate reservoirs: outline of a novel technique via a case study from the Molasse Basin, southern Bavaria, Germany, *Environmental Earth Sciences*, (2013), 1-18.

Cacas, M. C., Ledoux, E., de Marsily, G., Tillie, B., Barbreau, A., Durand, E., Feuga, B. & Peaudecerf, P.: Modeling fracture flow with a stochastic discrete fracture network: calibration and validation: 1. The flow model, *Water Resources Research*, *26*, (1990), 479-489.

Caumon, G., Collon-Drouaillet, P., Le Carlier de Veslud, C., Viseur, S. & Sausse, J.: Surface-based 3D modeling of geological structures, *Mathematical Geosciences,*, **41**, (2009), 927-945.

Chen, M., Buscheck, T., Wagoner, J., Sun, Y., White, J., Chiaramonte, L. & Aines, R.: Analysis of fault leakage from Leroy underground natural gas storage facility, Wyoming, USA, *Hydrogeology Journal,* **21**, (2013), 1429-1445.

Cherubini, Y., Cacace, M., Blöcher, G. & Scheck-Wenderoth, M.: Impact of single inclined faults on the fluid flow and heat transport: results from 3-D finite element simulations, *Environmental Earth Sciences*, (2013), 1-16.

Committee on Fracture Characterization and Fluid Flow, National Research Council: Rock Fractures and Fluid Flow: Contemporary Understanding and Applications, *The National Academies Press*, (1996).

Davatzes, N. & Aydin, A.: Distribution and nature of fault architecture in a layered sandstone and shale sequence: An example from the Moab fault, Utah, *AAPG Memoir*, (2005), 153-180.

Deshowitz, W. S.: Rock joint systems, *Massachusetts Institute of Technology. Dept. of Civil Engineering*, (1985).

Diersch H.-J.: FEFLOW Finite Element Subsurface Flow and Transport Simulation System – User's Manual/Reference Manual/ White Papers (2002), Release 5.0. WASY Ltd, Berlin.

Farmer, C.: Iske, A. & Randen, T.: (Eds.) Geological modelling and reservoir simulation, *Mathematical Methods and Modelling in Hydrocarbon Exploration and Production,* **7**, (2005), 119-212.

Graf, T. & Therrien, R.: A method to discretize non-planar fractures for 3D subsurface flow and transport simulations, *International Journal for Numerical Methods in Fluids,* **56**, (2008), 2069-2090.

Grisak, G. E. & Pickens, J. F.: Solute transport through fractured media: 1. The effect of matrix diffusion, *Water Resources Research*, **16**, (1980), 719-730.

Hofmann, H., Blöcher, G., Börsing, N., Maronde, N., Pastrik, N. & Zimmermann, G.: Potential for enhanced geothermal systems in low permeability limestones – stimulation strategies for the Western Malm karst (Bavaria), *Geothermics*, **51**, (2014), 351 - 367.

Holm, R., Kaufmann, R., Heimsund, B.-O., Øian, E. & Espedal, M. S.: Meshing of domains with complex internal geometries, *Numerical Linear Algebra with Applications,* **13**, (2006), 717-731.

Kolditz, O., Blöcher, M. G., Clauser, C., Diersch, H.-J. G., Kohl, T., Kühn, M., McDermott, C. I., Wang, W., Watanabe, N., Zimmermann, G. & Bruel, D.: Huenges, E.: (Ed.) Geothermal Energy Systems, Geothermal Reservoir Simulation, *Geothermal Energy Systems, Wiley*, (2010), 245-301.

Kolditz, O., Bauer, S., Bilke, L., Böttcher, N., Delfs, J.O., Fischer, T., Görke, U.J., Kalbacher, T., Kosakowski, G., McDermott, C.I., Park, C.H., Radu, F., Rink, K., Shao, H., Shao, HB., Sun, F., Sun, Y.Y., Singh, A.K., Taron, J., Walther, M., Wang, W., Watanabe, N., Wu, N., Xie, M., Xu, W., Zehner, B.: OpenGeoSys: an open-source initiative for numerical simulation of thermo-hydro-mechanical/chemical (THM/C) processes in porous media. *Environmental Earth Sciences,* 67(2), (2012), 589-599.

Magri, F., Bayer, U., Jahnke, C., Clausnitzer, V., Diersch, H.-J., Fuhrman, J., Möller, P., Pekdeger, A., Tesmer, M., Voigt HJ: Fluid-dynamics driving saline water in the North East German Basin. *International Journal of Earth Sciences*, **94**, (2005), 1056–69.

Mustapha, H. & Dimitrakopoulos, R.: Discretizing two-dimensional complex fractured fields for incompressible two-phase flow, *International Journal for Numerical Methods in Fluids*, **65**, (2011), 764-780.

Normani, S. D. & Sykes, J. F.: Paleoclimate analyses of density-dependent groundwater flow with pseudo-permafrost in discretely fractured crystalline rock settings, *XVIII International Conference on Water Resources -- CMWR 2010*, edited by J. Carrera, Barcelona, Spain, Jun. 21--24, (2010).

Prévost, M., Lepage, F., Durlofsky, L. J. & Mallet, J.-L.: Unstructured 3D gridding and upscaling for coarse modelling of geometrically complex reservoirs, *Petroleum Geoscience*, **11**, (2005), 339-345.

de Rooij, R.: Towards improved numerical modeling of karst aquifers: coupling turbulent conduit flow and laminar matrix flow under variably saturated conditions, *University of Neuchâtel*, (2008).

Shewchuk, J. R.: Delaunay refinement algorithms for triangular mesh generation, *Computational Geometry: Theory and applications*, **22**, (2002), 21-74.

Shikaze, S. G., Sudicky, E. & Schwartz, F.: Density-dependent solute transport in discretely-fractured geologic media: Is prediction possible?, *Journal of Contaminant Hydrology*, **34**, (1998), 273-291.

Si, H.: Three dimensional boundary conforming Delaunay mesh generation, *Technische Universität Berlin, Institut für Mathematik*, PhD Thesis, (2008)

Souche, L., Lepage, F. & Iskenova, G.: Volume based modeling - Automated construction of complex structural models, 75th EAGE Conference & Exhibition incorporating SPE EUROPEC 2013 London, UK, 10-13 June 2013, (2013).

Therrien, R. & Sudicky, E.: Three-dimensional analysis of variably-saturated flow and solute transport in discretely-fractured porous media, *Journal of Contaminant Hydrology*, **23**, (1996), 1-44.

Trice, R.: Application of borehole image logs in constructing 3D static models of productive fracture networks in the Apulian Platform, Southern Apennines, *Geological Society, London, Special Publications*, **159**, (1999), 155-176.

Watanabe, N., Wang, W., Taron, J., Gorke, U.-J., Kolditz, O.: Lower-dimensional interface elements using local enrichments and application for a coupled hydromechanical problem in fractured rock. *International Journal for Numerical Methods in Engineering*, 90(8), (2012), 1010-1034.

Zimmermann, G., Moeck, I. & Blöcher, G.: Cyclic waterfrac stimulation to develop an Enhanced Geothermal System (EGS) - Conceptual design and experimental results, *Geothermics*, **39**, (2010), 59-69.

Zimmermann, G., Tischner, T., Legarth, B. & Huenges, E.: Pressure-dependent production efficiency of an Enhanced Geothermal System (EGS): Stimulation results and implications for hydraulic fracture treatments, *Pure and Applied Geophysics*, **166**, (2009), 1089-1106.